

Tests of Lepton Flavour Universality and searches for Lepton Flavour Violation at LHCb

Alessandra Gioventù^{a,*}

^a*Instituto Galego de Física de Altas Enerxías (IGFAE), Universidade de Santiago de Compostela, Rúa de Xoaquín Díaz de Rábago s/n, Santiago de Compostela, Spain*

E-mail: alessandra.gioventu@cern.ch

An embedded feature of the Standard Model is that different charged leptons have the same interaction strengths with the electroweak-force carriers. This is known as Lepton Flavour Universality (LFU). The LFU is an accidental symmetry of the SM, not the result of some fundamental underlying principle. Recent results on LFU tests in semileptonic $b \rightarrow c\ell\nu$ transitions and rare $b \rightarrow s\ell\ell$ decays, point to a violation of the LFU. If confirmed by further measurements, this would be clear evidence of New Physics in which new heavy particles couple preferentially to 2nd or 3rd generations of leptons. Many extensions of the SM that include violation of the LFU, predict Lepton Flavour Violating (LFV) processes in hadron decays with charged leptons in the final state. In this talk, the recent results from LHCb on LFU tests along with searches of charged-LFV are reported.

*7th Symposium on Prospects in the Physics of Discrete Symmetries (DISCRETE 2020-2021)
29th November - 3rd December 2021
Bergen, Norway*

¹On behalf of the LHCb Collaboration

*Speaker

1. Introduction

The Standard Model (SM) of particle physics organises leptons and quarks in three families or generations, distinguished only by their masses. The SM assumes that the couplings between leptons and electroweak gauge bosons (Z^0, W^\pm) are independent of the generation. This property is known as Lepton Flavour Universality (LFU). Many new physics (NP) scenarios foresee LFU-violating processes, involving mostly the third generation [1]. Results from tests of LFU raised the interest also in searches of Lepton Flavour Violating (LFV) decays. In these processes lepton number conservation is directly violated, which would be a direct indication of NP.

The LHCb experiment [2] is dedicated to perform heavy flavour physics measurements and it is an excellent place to search for indirect evidences of NP. The LHCb experiment collected data from proton-proton collisions in two runs, with different conditions: Run 1 (2010-2012), with a centre-of-mass energy, \sqrt{s} , of 7 and 8 TeV, and Run 2 (2015-2018) with $\sqrt{s} = 13$ TeV. The combination of the two data samples corresponds to an integrated luminosity of 9 fb^{-1} , 3 and 6 fb^{-1} respectively.

2. Lepton Flavour Universality tests at LHCb

The recent experimental results on b-hadron decays have shown some tensions with the SM expectations. These measurements have been obtained studying two different quark transitions: $b \rightarrow c\ell\nu_\ell$ and $b \rightarrow s\ell\ell$. In the SM, $b \rightarrow c\ell\nu_\ell$ transitions, where $\ell = \tau, \mu$, are tree-level processes, mediated by a W boson with a branching fraction of the order of a few percent. The other set of measurements involves $b \rightarrow s\ell\ell$ transitions, where $\ell = e, \mu$. In the SM these are Flavour Changing Neutral Currents (FCNC) processes, occurring only at the loop level: through a box diagram with two W bosons or a penguin diagram with the exchange of a γ or a Z boson. Hence $b \rightarrow c\ell\nu_\ell$ and $b \rightarrow s\ell\ell$ transitions are sensitive to NP at tree or loop level.

It is possible to use various observables to probe LFU: angular observables, differential decay rates and ratios of observables. The latter are defined as the ratio of the branching fractions of decays involving leptons from different generations $R(H)$ and they are the focus of this report.

2.1 $b \rightarrow c\ell\nu_\ell$ transitions

The ratio $R(H_c)$ is defined as

$$R(H_c) = \frac{BR(H_b \rightarrow H_c \tau^- \bar{\nu}_\tau)}{BR(H_b \rightarrow H_c \mu^- \bar{\nu}_\mu)}, \quad \text{where } H_c = D^*, D^+, J/\psi, \Lambda_c^+ \dots \text{ and } H_b = B^\pm, B^0, B_c^+, \Lambda_b^0. \quad (1)$$

Due to the different lepton masses, $R(H_c)$ deviates from unity in the SM, *i.e.* $R(D) = 0.298 \pm 0.003$, $R(D^*) = 0.252 \pm 0.005$ [3]. The experimental measurements of $R(D)$ and $R(D^*)$ show some tensions from the expected values, $\sim 1.4\sigma$ and $\sim 2.5\sigma$ respectively [3]. The combined $R(D)$ and $R(D^*)$ measurements, taking into account the correlations among measurements, show an overall tension of about 3.4σ , as shown in Fig. 1.

At the LHCb experiment [2], $b \rightarrow c\tau\nu$ processes display two main challenges due to the presence of at least one neutrino in the final state. First of all, the kinematical constraints used by Belle and BaBar cannot be exploited in the reconstruction. Likewise, due to the design of

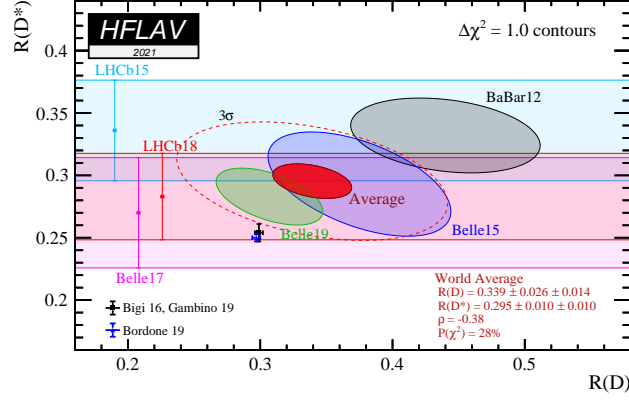


Figure 1: Average of the ratios and comparison with SM predictions [3]. Measurements of $R(D)$ and $R(D^*)$ performed by BaBar [4–7], Belle [8, 9] and LHCb [10–12]. The SM predictions are the black [13, 14] and blue [15] crosses, the simultaneous measurements are represented as ellipses while $R(D^*)$ only are the horizontal bands.

the detector, the same estimation strategies adopted by 4π detector at hadronic colliders, such as the missing transverse energy, cannot be used. In $R(H_c)$ analyses at LHCb, two different decay channels are considered to study the tau lepton: the muonic $\tau^- \rightarrow \mu^- \bar{\nu}_\mu \nu_\tau$ and the hadronic $\tau^- \rightarrow \pi^- \pi^+ \pi^- \nu_\tau$ decay modes. Thus, a normalisation channel is chosen so that both normalisation and the signal have the same visible final state, and systematic uncertainties cancel in the ratio.

All the $R(H_c)$ measurements reported here are carried out using the Run 1 data sample (3 fb^{-1}).

2.1.1 Muonic $R(H_c)$ measurements

For muonic $R(H_c)$ measurements a kinematical approximation of the B momentum is used [10, 16]. The first $R(D^*)$ measurement by LHCb was performed using the $\bar{B}^0 \rightarrow D^{*+} \ell^- \bar{\nu}_\ell$ decay, where the D^{*+} is reconstructed through the decay $D^{*+} \rightarrow D^0 (\rightarrow K^- \pi^+) \pi^+$ [10]. The final result is $R(D^*) = 0.366 \pm 0.027$ (stat.) ± 0.030 (syst.). The main contribution to the systematic uncertainties is due to the size of the simulation sample.

A measurement of $R(J/\psi)$ is performed with $B_c^+ \rightarrow J/\psi \ell^+ \nu_\ell$ decays. The final result is $R(J/\psi) = 0.71 \pm 0.17$ (stat.) ± 0.18 (syst.) [16]. The main systematic uncertainties are due to the size of the B_c^+ simulation sample and the poor knowledge of the form factors involved in these semileptonic decays.

2.1.2 Hadronic $R(D^*)$ measurement

The first measurement of $R(D^*)$ using the 3-prong final state, $\tau^+ \rightarrow \pi^+ \pi^- \pi^+ (\pi^0) \bar{\nu}_\tau$, has been published by LHCb [11, 12]. The measured quantity is

$$K(D^{*-}) = \frac{BR(B^0 \rightarrow D^{*-} \tau^+ \nu_\tau)}{BR(B^0 \rightarrow D^{*-} \pi^+ \pi^- \pi^+)}. \quad (2)$$

Thus, $R(D^{*-})$ is obtained as $R(D^{*-}) = K(D^{*-}) \times (BR(B^0 \rightarrow D^{*-} \pi^+ \pi^- \pi^+) / BR(B^0 \rightarrow D^{*-} \mu^+ \nu_\mu))$, where the branching fractions of $B^0 \rightarrow D^{*-} 3\pi$ and $B^0 \rightarrow D^{*-} \mu^+ \nu_\mu$ are averages from external measurements [17].

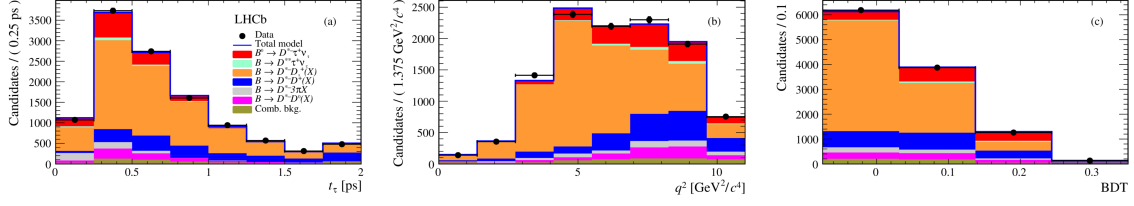


Figure 2: Projections of the three-dimensional fit to extract signal yields [11, 12]. From left to right, distributions of the τ decay time t_τ , the transfer momentum q^2 and the BDT output. The signal $B^0 \rightarrow D^{*-}\tau^+\nu_\tau$ component is represented in red, $B^0 \rightarrow D^{*-}D_s^+(X)$ channel in orange and other different components are represented with different colours.

The yield of the normalisation channel is obtained from an unbinned maximum likelihood fit to the invariant mass $M(D^{*-}\pi^+\pi^-\pi^+)$. The signal yield is extracted from a 3-dimensional fit to data, where the variables are the momentum transferred to the τ - ν system, q^2 , the τ decay time t_τ and the output of a multivariate classifier (BDT) (Fig. 2). The measured value is $R(D^*) = 0.291 \pm 0.019$ (stat.) ± 0.026 (syst.) ± 0.013 (ext.).

2.2 $b \rightarrow s\ell^-\ell^+$ transitions

For FCNC transitions, within a given range of the dilepton invariant mass squared q^2 , the ratio of observables are defined as

$$R(H_s)[q_{min}^2, q_{max}^2] = \frac{\int_{q_{min}^2}^{q_{max}^2} dq^2 \frac{d\Gamma(H_b \rightarrow H_s \mu^+ \mu^-)}{dq^2}}{\int_{q_{min}^2}^{q_{max}^2} dq^2 \frac{d\Gamma(H_b \rightarrow H_s e^+ e^-)}{dq^2}} \quad (3)$$

where H_b and H_s stand for a b and s hadron respectively. The main challenge of these measurements is the presence of the electrons in the final state. Since they lose energy through bremsstrahlung radiation, the ratio of Eq. 3 does not cancel completely the systematic uncertainties. This is in part solved considering the double ratio of Eq. 4, exploiting the proprieties of the control modes $J/\psi \rightarrow \ell^+\ell^-$: the BR s ratio is known to be unity and the values of BR s are known with very good precision. Moreover, the topology of $J/\psi \rightarrow \ell^+\ell^-$ and the non-resonant channels are similar.

$$R(H_s) = \frac{BR(H_b \rightarrow H_s \mu^+ \mu^-)}{BR(H_b \rightarrow H_s J/\psi(\rightarrow \mu^+ \mu^-))} \Bigg/ \frac{BR(H_b \rightarrow H_s e^+ e^-)}{BR(H_b \rightarrow H_s J/\psi(\rightarrow e^+ e^-))}. \quad (4)$$

In addition, to improve the energy resolution and take into account the bremsstrahlung photons, a recovery procedure is performed. For each electron track, showers in the electronic calorimeter (ECAL) that are not associated with any other charged tracks in the ECAL are searched around the extrapolated track direction before and after the magnet.

Finally, the yields are extracted from a simultaneous fit to the H_b mass distribution $M(H_s \ell^+ \ell^-)$ of the resonant and non-resonant channels.

The following $R(H_s)$ measurements, when not specified, are performed with the full LHCb data sample, corresponding to an integrated luminosity of 9 fb^{-1} .

2.2.1 $R(K)$ measurement

The $B^+ \rightarrow K^+ \ell^+ \ell^-$ decay is studied to measure $R(K)$ in the q^2 range $1.1 - 6.0 \text{ GeV}^2/c^4$ [18]. The fit results are represented in Fig. 3. The main contributions to the background are due to the

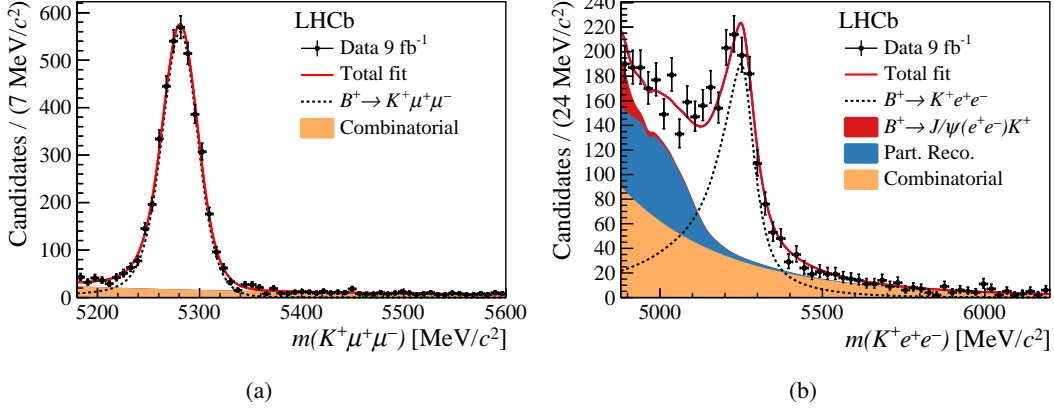


Figure 3: $M(K\ell^+\ell^-)$ distributions after the fit for the μ (left) and e (right) non-resonant final states [18]. The fit result is represented by the red line, while the signal component by the black dotted line and the remaining colours represent the different sources of background.

combinatorial background, which is higher in the electronic final state and the partially reconstructed $K^{*+}e^+e^-$. The final result is $R(K) = 0.846^{+0.042}_{-0.039}(\text{stat.})^{+0.013}_{-0.012}(\text{syst.})$. The compatibility with respect to the SM prediction is 3.1σ .

2.2.2 $R(K_S^0)$ and $R(K^{*+})$ measurements

The latest publication on $R(H_s)$ aims to probe LFU using $B^0 \rightarrow K_S^0 \ell^+ \ell^-$ and $B^+ \rightarrow K^{*+} \ell^+ \ell^-$ decays [19]. Kaons are reconstructed by the $K_S^0 \rightarrow \pi^+ \pi^-$ and $K^{*+} \rightarrow K_S^0 \pi^+$ decays. This is the first observation of the $B^0 \rightarrow K_S^0 e^+ e^-$ (Fig. 4(b)) and $B^+ \rightarrow K^{*+} e^+ e^-$ (Fig. 4(d)) decays for $1.1 < q^2 < 6.0 \text{ GeV}^2/c^4$ and $0.045 < q^2 < 6.0 \text{ GeV}^2/c^4$, respectively. The final results are $R(K_S^0) = 0.66^{+0.20}_{-0.14}(\text{stat.})^{+0.02}_{-0.04}(\text{syst.})$ and $R(K^{*+}) = 0.70^{+0.18}_{-0.13}(\text{stat.})^{+0.03}_{-0.04}(\text{syst.})$ in the respective q^2 regions, in the agreement with the SM at the level of 1.5σ and 1.4σ .

2.2.3 Other ratio measurements on $b \rightarrow s \ell \ell$ transitions

Many decay channels have been investigated by the LHCb. The first measurement on these transitions, with Run I data is $R(K^{*0})$ in two q^2 regions ($[0.045, 1.1]$ and $[1.1, 6.0] \text{ GeV}^2/c^4$) [20]: $R(K^{*0}) = 0.66^{+0.11}_{-0.07} \pm 0.03$, $R(K^{*0}) = 0.69^{+0.11}_{-0.07} \pm 0.05$. Finally, another probe of LFU has been performed with Run 1+2 sample [21]. The $\Lambda_b^0 \rightarrow p K \ell^+ \ell^-$ decay is studied for $0.1 < q^2 < 6.0 \text{ GeV}^2/c^4$, obtaining $R(pK) = 0.86^{+0.14}_{-0.11}(\text{stat.}) \pm 0.05(\text{syst.})$, compatible with the SM prediction within one standard deviation.

3. Searches for LFV decays

Lepton Flavour Violating decays are highly suppressed in the SM. Both leptonic and semileptonic final states have been investigated by LHCb. Most of the limits reported here refers to Run 1 data sample (3 fb^{-1}) when not specified.

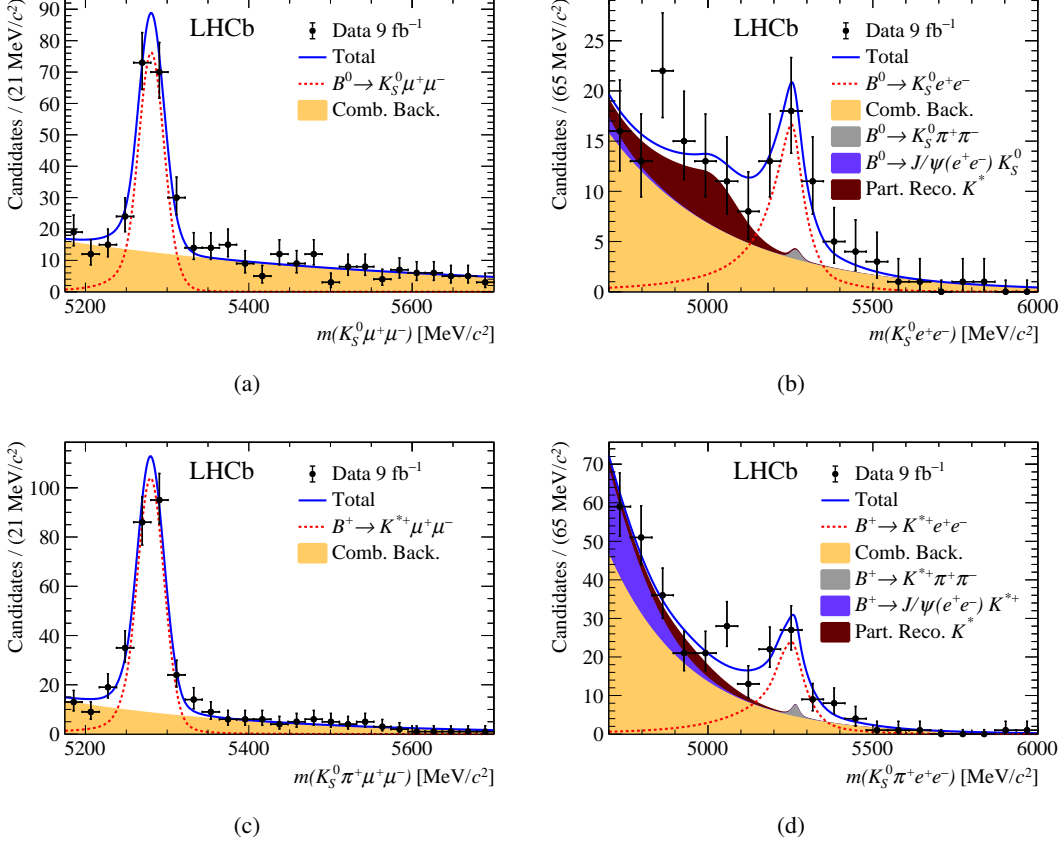


Figure 4: Invariant mass distributions of $M(K_S^0 \ell^+ \ell^-)$ (top) and $M(K_S^0 \pi^+ \ell^+ \ell^-)$ (bottom) after the fit for the non-resonant final states [19]. Muon mode on the left and electron mode on the right. The fit result is represented by the blue line, while the signal component by the red dotted line and the remaining colours represent the different sources of background.

3.1 $\mu\tau$ final states

As stated before, in the LHCb experiment taus can be reconstructed exploiting different decay channels. Three-prong tau decays, $\tau \rightarrow 3\pi\nu_\tau$, are used to search for LFV, as in [22]. This study set upper limits for $B_S^0 \rightarrow \tau^\pm \mu^\mp$ without any $B^0 \rightarrow \tau^\pm \mu^\mp$ contribution and likewise for the B^0 decay, obtaining $BR(B_S^0 \rightarrow \tau^\pm \mu^\mp) < 4.2 \times 10^{-5}$ and $BR(B^0 \rightarrow \tau^\pm \mu^\mp) < 1.4 \times 10^{-5}$ at 95% confidence level [22].

$B^+ \rightarrow K^+ \mu^- \tau^+$ decays are investigated by using a reconstruction method complementary to the three-prong τ decays one, which is employed in a dedicated ongoing analysis. In [23] taus are reconstructed by tagging the B from prompt $B_{s2}^{*0} \rightarrow B^+ K^-$ decays, allowing to take into account of the neutrino by the missing 4-momentum as $P_{\text{miss}} = P_B - P_{K\mu}$. The upper limit on the rate of the LFV decay $B^+ \rightarrow K^+ \mu^- \tau^+$ is set to 4.5×10^{-5} at 95%CL.

3.2 μe final states

Searches for LFV with an electron and a muon in the final state have been performed by the LHCb experiment in various channels. In [24] upper limits are set to $BR(B_S^0 \rightarrow e^\pm \mu^\mp) < 5.4(6.3) \times$

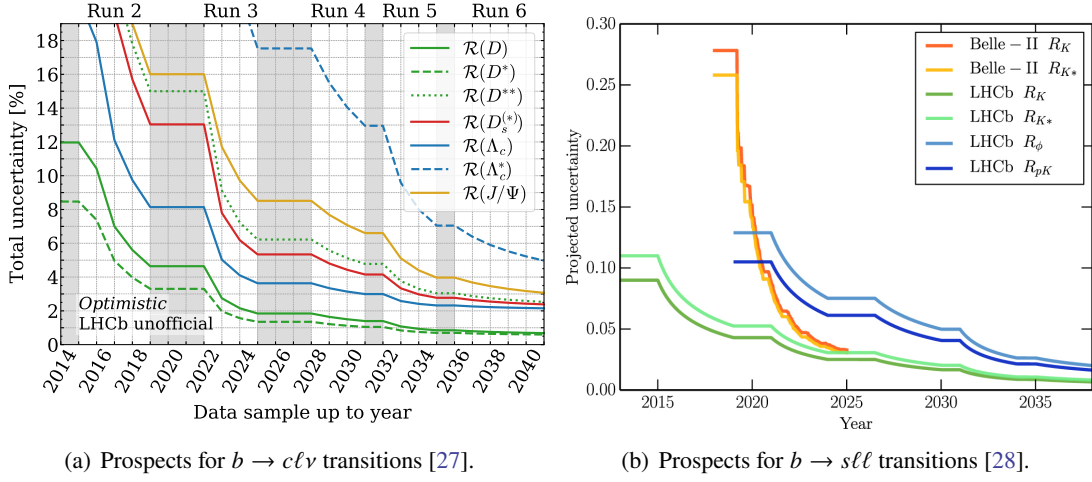


Figure 5: Left: expected precision on the measurement of $R(H_c)$ ratios at LHCb as a function of the year for irreducible systematic uncertainty of 0.5% on $R(D^{(*)})$ and 2% on the other ratios from [27]. Right: expected precision on the measurement of $R(H_s)$ ratios in function of the year at LHCb and Belle II [28].

10^{-9} and $BR(B^0 \rightarrow e^\pm\mu^\mp) < 1.3 \times 10^{-9}$ at 95% confidence level. Moreover, limits to the decay rate of $B^+ \rightarrow K^+\mu^\pm e^\mp$ are set to $BR(B^+ \rightarrow K^+e^-\mu^+) < 9.5 \times 10^{-9}$ and $BR(B^+ \rightarrow K^+e^+\mu^-) < 8.8 \times 10^{-9}$ at 95% CL [25]. Finally, other searches for LFV have been performed with charm meson decays of the type $D_{(s)}^+ \rightarrow h^\pm\ell^+\ell'^\mp$, where $h = K, \pi$ and $\ell = \mu, e$. Upper limits are set between 1.4×10^{-8} and 6.4×10^{-6} [26].

4. Conclusions and future prospects

Tests of LFU show tensions with the SM predictions in both tree-level and FCNC transitions. In Fig. 5 the prospects for LFU tests with $b \rightarrow c\ell\nu$ (Fig. 5(a)) and $b \rightarrow s\ell\ell$ (Fig. 5(b)) transitions are reported. As of today, the experimental results on the combination of $R(D)$ and $R(D^*)$ show a discrepancy with respect to the SM of ~ 3.4 standard deviations and the $R(K)$ measurement differs from the SM prediction by $\sim 3.1\sigma$. The uncertainties in ratio measurements are expected to improve for different reasons. Firstly, complementary studies on the form factor parameters and the branching fractions of background decay channels are being carried out. These give fundamental inputs to future measurements of both LFU tests and searches for LFV. Moreover, LHCb is undergoing an upgrade towards Run 3, which will start in 2022. The LHCb Upgrade I detector is expected to collect data corresponding to an integrated luminosity of 25 fb^{-1} . Studying this new sample and using the full Run 1+Run 2 one, will reduce LHCb statistical uncertainties and data driven systematic uncertainties [27, 28].

To adapt to the new run conditions, major improvements are made in selection and reconstruction at the LHCb Upgrade I detector. A new trigger strategy and an upgraded tracking system are implemented, which will improve analyses with more than one decay vertex.

References

- [1] S. Fajfer, J. F. Kamenik and I. Nisandzic, *On the $B \rightarrow D^* \tau \bar{\nu}_\tau$ sensitivity to new physics*, *Phys. Rev.* **D85** (2012) 094025 [1203.2654].
- [2] LHCb collaboration, *The LHCb detector at the LHC*, *JINST* **3** (2008) S08005.
- [3] HEAVY FLAVOR AVERAGING GROUP collaboration, *Averages of b -hadron, c -hadron, and τ -lepton properties as of 2018*, *Eur. Phys. J.* **C81** (2021) 226 [1909.12524].
- [4] BELLE collaboration, *Measurement of the branching ratio of $\bar{B} \rightarrow D^{(*)} \tau^- \bar{\nu}_\tau$ relative to $\bar{B} \rightarrow D^{(*)} \ell^- \bar{\nu}_\ell$ decays with hadronic tagging at Belle*, *Phys. Rev. D* **92** (2015) 072014 [1507.03233].
- [5] BELLE collaboration, *Measurement of the branching ratio of $\bar{B}^0 \rightarrow D^{*+} \tau^- \bar{\nu}_\tau$ relative to $\bar{B}^0 \rightarrow D^{*+} \ell^- \bar{\nu}_\ell$ decays with a semileptonic tagging method*, *Phys. Rev. D* **94** (2016) 072007 [1607.07923].
- [6] BELLE collaboration, *Measurement of the τ lepton polarization and $R(D^*)$ in the decay $\bar{B} \rightarrow D^* \tau^- \bar{\nu}_\tau$* , *Phys. Rev. Lett.* **118** (2017) 211801 [1612.00529].
- [7] BELLE collaboration, *Measurement of $\mathcal{R}(D)$ and $\mathcal{R}(D^*)$ with a semileptonic tagging method*, 1904.08794.
- [8] BABAR collaboration, *Evidence for an excess of $\bar{B} \rightarrow D^{(*)} \tau^- \bar{\nu}_\tau$ decays*, *Phys. Rev. Lett.* **109** (2012) 101802 [1205.5442].
- [9] BABAR collaboration, *Measurement of an Excess of $\bar{B} \rightarrow D^{(*)} \tau^- \bar{\nu}_\tau$ Decays and Implications for Charged Higgs Bosons*, *Phys. Rev. D* **88** (2013) 072012 [1303.0571].
- [10] LHCb collaboration, *Measurement of the ratio of branching fractions $\mathcal{B}(\bar{B}^0 \rightarrow D^{*+} \tau^- \bar{\nu}_\tau) / \mathcal{B}(\bar{B}^0 \rightarrow D^{*+} \mu^- \bar{\nu}_\mu)$* , *Phys. Rev. Lett.* **115** (2015) 111803 LHCb-PAPER-2015-025, CERN-PH-EP-2015-150, [1506.08614].
- [11] LHCb collaboration, *Measurement of the ratio of the $\mathcal{B}(B^0 \rightarrow D^{*-} \tau^+ \nu_\tau)$ and $\mathcal{B}(B^0 \rightarrow D^{*-} \mu^+ \nu_\mu)$ branching fractions using three-prong τ -lepton decays*, *Phys. Rev. Lett.* **120** (2018) 171802 LHCb-PAPER-2017-017, CERN-EP-2017-212, [1708.08856].
- [12] LHCb collaboration, *Test of lepton flavor universality by the measurement of the $B^0 \rightarrow D^{*-} \tau^+ \nu_\tau$ branching fraction using three-prong τ decays*, *Phys. Rev.* **D97** (2018) 072013 LHCb-PAPER-2017-027, CERN-EP-2017-256, [1711.02505].
- [13] D. Bigi and P. Gambino, *Revisiting $B \rightarrow D \ell \nu$* , *Phys. Rev. D* **94** (2016) 094008 [1606.08030].
- [14] P. Gambino, M. Jung and S. Schacht, *The V_{cb} puzzle: An update*, *Phys. Lett. B* **795** (2019) 386 [1905.08209].

- [15] M. Bordone, M. Jung and D. van Dyk, *Theory determination of $\bar{B} \rightarrow D^{(*)} \ell^- \bar{\nu}$ form factors at $\mathcal{O}(1/m_c^2)$* , *Eur. Phys. J. C* **80** (2020) 74 [1908.09398].
- [16] LHCb collaboration, *Measurement of the ratio of branching fractions $\mathcal{B}(B_c^+ \rightarrow J/\psi \tau^+ \nu_\tau)/\mathcal{B}(B_c^+ \rightarrow J/\psi \mu^+ \nu_\mu)$* , *Phys. Rev. Lett.* **120** (2018) 121801 LHCb-PAPER-2017-035, CERN-EP-2017-275, [1711.05623].
- [17] PARTICLE DATA GROUP collaboration, *Review of Particle Physics*, *PTEP* **2020** (2020) 083C01.
- [18] LHCb collaboration, *Test of lepton universality in beauty-quark decays*, *Nature Phys.* **18** (2022) 277 LHCb-PAPER-2021-004, CERN-EP-2021-042, [2103.11769].
- [19] LHCb collaboration, *Tests of lepton universality using $B^0 \rightarrow K_S^0 \ell^+ \ell^-$ and $B^+ \rightarrow K^{*+} \ell^+ \ell^-$ decays*, **2110.09501** LHCb-PAPER-2021-038, CERN-EP-2021-208, [2110.09501].
- [20] LHCb collaboration, *Test of lepton universality with $B^0 \rightarrow K^{*0} \ell^+ \ell^-$ decays*, *JHEP* **08** (2017) 055 LHCb-PAPER-2017-013, CERN-EP-2017-100, [1705.05802].
- [21] LHCb collaboration, *Test of lepton universality using $\Lambda_b^0 \rightarrow p K^- \ell^+ \ell^-$ decays*, *JHEP* **05** (2020) 040 LHCb-PAPER-2019-040 CERN-EP-2019-272, [1912.08139].
- [22] LHCb collaboration, *Search for the lepton-flavour-violating decays $B_s^0 \rightarrow \tau^\pm \mu^\mp$ and $B^0 \rightarrow \tau^\pm \mu^\mp$* , *Phys. Rev. Lett.* **123** (2019) 211801 LHCb-PAPER-2019-016 CERN-EP-2019-076, [1905.06614].
- [23] LHCb collaboration, *Search for the lepton flavour violating decay $B^+ \rightarrow K^+ \mu^- \tau^+$ using B_{s2}^{*0} decays*, *JHEP* **06** (2020) 129 LHCb-PAPER-2019-043 CERN-EP-2020-020, [2003.04352].
- [24] LHCb collaboration, *Search for the lepton-flavour violating decays $B_{(s)}^0 \rightarrow e^\pm \mu^\mp$* , *JHEP* **03** (2018) 078 LHCb-PAPER-2017-031 CERN-EP-2017-242, [1710.04111].
- [25] LHCb collaboration, *Search for the lepton-flavour violating decays $B^+ \rightarrow K^+ \mu^\pm e^\mp$* , *Phys. Rev. Lett.* **123** (2019) 231802 LHCb-PAPER-2019-022 CERN-EP-2019-172, [1909.01010].
- [26] LHCb collaboration, *Searches for 25 rare and forbidden decays of D^+ and D_s^+ mesons*, *JHEP* **06** (2021) 044 LHCb-PAPER-2020-007, CERN-EP-2020-140, [2011.00217].
- [27] F. U. Bernlochner, M. Franco Sevilla, D. J. Robinson and G. Wormser, *Semitaquonic b -hadron decays: A lepton flavor universality laboratory*, **2101.08326**.
- [28] S. Bifani, S. Descotes-Genon, A. Romero-Vidal and M.-H. Schune, *Review of lepton universality tests in b decays*, *Journal of Physics G: Nuclear and Particle Physics* **46** (2018) 023001.